Huang, C. C., Hearst, J., & Alberts, B. (1981) *J. Biol. Chem. 256*, 4087-4094.
Isaacs, S., Wiesehahn, G., & Hallick, L. (1984) *Natl. Cancer Inst. Monogr. 66*, 21-31.
Kanne, D., Straub, K., Rapoport, H., & Hearst, J. (1982) *Biochemistry 21*, 861-871.
Koffel-Schwartz, N., Verdier, J. M., Bichara, M., Freund, A. M., Daune, M., & Fuchs, R. P. P. (1984) *J. Mol. Biol. 177*, 33-51.
Macino, G., & Tzagoloff, A. (1980) *Cell (Cambridge, Mass.) 20*, 507-517.
Magaña-Schwencke, N., & Moustacchi, E. (1985) *Photochem. Photobiol. 42*, 43-49.
Maxam, A., & Gilbert, W. (1980) *Methods Enzymol. 65*, 499-560.
McClellan, J. A., Palecek, E., & Lilley, D. (1986) *Nucleic Acids Res. 14*, 9291-9309.
Miller, S., & Eisenstadt, E. (1987) *J. Bacteriol. 169*, 2724-2729.
Moysan, A. (1987) Ph.D. Thesis, Université Pierre et Marie Curie, Paris, France.
Nocentini, S. (1986) *Mutat. Res. 161*, 181-192.
Papadopoulo, D., Averbeck, D., & Moustacchi, E. (1986) *Photochem. Photobiol. 44*, 31-39.
Pearlman, D., Holbrook, S., Pirkle, D., & Kim, S. H. (1985) *Science (Washington, D.C.) 227*, 1304-1308.
Piette, J., Decuyper-Debergh, D., & Gamper, H. (1985) *Proc. Natl. Acad. Sci. U.S.A. 82*, 7355-7359.
Sage, E. (1981) Ph.D. Thesis, Université d'Orléans, Orléans, France.
Sage, E., & Leng, M. (1980) *Proc. Natl. Acad. Sci. U.S.A. 77*, 4597-4601.
Sage, E., & Moustacchi, E. (1987) *Biochemistry 26*, 3307-3314.
Shi, Y., & Hearst, J. (1986) *Biochemistry 25*, 5895-5902.
Sinden, R. R., & Hagerman, P. J. (1984) *Biochemistry 23*, 6299-6303.
Smith, C. A. (1987) in *Psoralen DNA Photobinding* (Gasparro, F. P., Ed.) CRC Press, Boca Raton, FL (in press).
Sobell, H. M., Sakore, T. D., Jain, S. C., Banerjee, K. K., Bhandary, K. K., Reddy, B. S., & Lozansky, E. D. (1982) *Cold Spring Harbor Symp. Quant. Biol. 47*, 293-314.
Straub, K., Kanne, D., Hearst, J., & Rapoport, H. (1981) *J. Am. Chem. Soc. 103*, 2347-2355.
Vigny, P., Blais, J., Ibanez, V., & Geacintov, N. (1987) *Photochem. Photobiol. 45*, 601-607.
Waye, J. S., & Willard, H. F. (1986) *Mol. Cell. Biol. 6*, 3156-3165.
Wiesehahn, G., & Hearst, J. (1978) *Proc. Natl. Acad. Sci. U.S.A. 75*, 2703-2707.
Yatagai, F., & Glickman, B. W. (1986) *Mutat. Res. 163*, 209-224.
Yatagai, F., Horsfall, M. J., & Glickman, B. W. (1987) *J. Mol. Biol. 194*, 601-607.

Interaction of Synthetic Analogues of Distamycin and Netropsin with Nucleic Acids. Does Curvature of Ligand Play a Role in Distamycin–DNA Interactions?†

K. Ekambareswara Rao, Dipak Dasgupta,‡ and V. Sasisekharan*
Molecular Biophysics Unit, Indian Institute of Science, Bangalore 560 012, India
Received July 27, 1987; Revised Manuscript Received December 11, 1987

ABSTRACT: Distamycin and netropsin, a class of minor groove binding nonintercalating agents, are characterized by their B-DNA and A-T base-specific interactions. To understand the conformational and chemical basis of the above specificities, the DNA-binding characteristics of a novel synthetic analogue of distamycin have been studied. The analogue, mPD derivative, has the requisite charged end groups and a number of potential hydrogen-bonding loci equal to those of distamycin. The difference in the backbone curvatures of the ligands, distamycin, the mPD derivative, and NSC 101327 (another structurally analogous compound), is a major difference between these ligands. UV and CD spectroscopic studies reported here show the following salient features: The mPD derivative recognizes only B-DNA, to which it binds via the minor groove. On the other hand, unlike distamycin, it binds with comparable affinities to A-T and G-C base pairs in a natural DNA. These DNA-binding properties are compared with those reported earlier for distamycin and NSC 101327 [Zimmer, Ch., & Wahnert, U. (1986) *Prog. Biophys. Mol. Biol. 47*, 31-112]. The backbone structures of these three ligands were compared to show the progressive decrease in curvatures in the order distamycin, mPD derivative, and NSC 101327. The plausible significance of the backbone curvature vis-à-vis the characteristic B-DNA and AT-specific binding of distamycin is discussed. To our knowledge, this is the first attempt (with a model synthetic analogue) to probe the possible influence of backbone curvature upon the specificity of interactions of the distamycin class of groove-binding ligands with DNA.

The binding of the class of minor groove binding nonintercalating antibiotics, like distamycin (Dst) and netropsin (Nt), to synthetic and natural DNAs has evoked much interest in view of its significance in understanding the elements of specific recognition between nonintercalating ligands and DNA (Zimmer & Wahnert, 1986). X-ray crystallographic studies and the physicochemical investigations in solutions have indicated that the A-T base-specific and B-DNA selective nature of binding of Dst (and Nt) might be ascribed to electrostatic, van der Waals, and hydrogen-bonding interactions (Kopka et al., 1985; Zimmer & Wahnert, 1986). The theoretical cal-

† This work was supported by Grant ICMR/MBU/VS/24 from the Indian Council of Medical Research. K.E.R. is a recipient of a research associateship from the Council of Scientific and Industrial Research, India.
* Author to whom correspondence should be addressed.
‡ Present address: Crystallography and Molecular Biology Division, Saha Institute of Nuclear Physics, Bidhannagar, Calcutta 700 064, India.

0006-2960/88/0427-3018$01.50/0

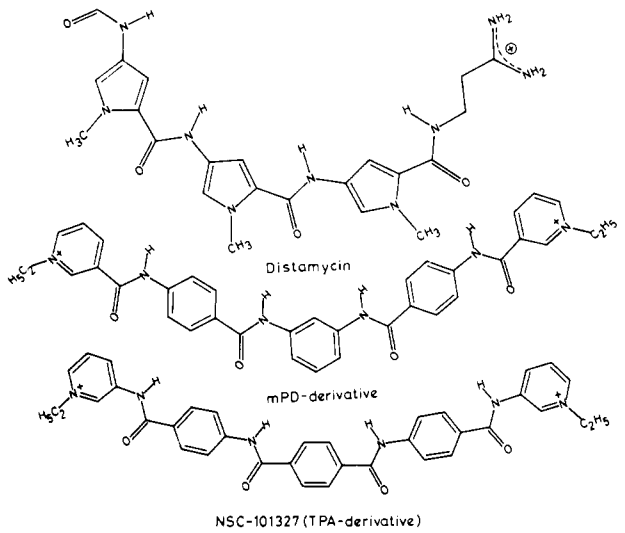

FIGURE 1: Computer-drawn structures of Dst, mPD derivative, and the synthetic ligands, a *m*-phenylenediamine derivative (abbreviated as mPD derivative) and NSC 101327 [a terephthalic acid derivative, first reported by Atwell and Cain (1968)]. The structures of mPD derivative and NSC 101327 are generated by using standard bond lengths and angles obtained from crystal geometry data of the constituent moieties. In the case of Dst, the reported bond lengths and angles for the crystal structure of Nt have been used.

culations to understand the specificity have indicated that the negative electrostatic potential within the minor groove might play an important role in the observed A-T specificity. Thus, it seems that if a relatively good steric fit can be obtained in the minor groove, the ligand will be sufficiently stabilized there by the favorable electrostatic potentials and Lennard-Jones energy terms (Pullman, 1986). There have been recent reports of experimental studies also with various Dst and Nt analogues (Lown et al., 1986; Wade & Dervan, 1987) to understand the molecular basis of interactions between these drugs and DNA. However, the roles of (1) the backbone curvature of ligands in favoring the noncovalent interactions and (2) extensive delocalization of π electrons via the presence of consecutive *N*-methylpyrrole rings upon the conformational and chemical specificity of the binding are yet to be understood. In our laboratory, we are studying the interactions of various synthetic analogues of Dst (and Nt) to throw light on the possible roles of these two structural features in the A-T-specific nature of their interactions with DNA (Dasgupta et al., 1986, 1987; Parrack et al., 1987). It was shown in an earlier report that the disruption of the delocalization of π electrons (via the contiguous pyrrole moieties in Dst) by insertion of a saturated β-alanine moiety as a substitute for the middle or terminal pyrrole moiety in Dst does not alter the A-T base specificity of the ligands, while it leads to a decrease in the stability of the complex with DNA (Parrack et al., 1987; Dasgupta et al., 1987).

To probe the role of curvature of the ligand in the selectivity, the DNA-binding characteristics of a Dst analogue containing benzene rings instead of the pyrrole rings was reported from this laboratory (Dasgupta et al., 1986). In this paper, we report the results of DNA-binding characteristics of another type of ligand containing bisquaternary ammonium heterocycles (structure shown in Figure 1). This new ligand, a derivative of *m*-phenylenediamine (mPD), is, to a degree, structurally analogous to the reported antileukemic compound NSC 101327, a derivative of terephthalic acid (Atwell & Cain, 1968; Luck et al., 1984). The chemical structure of this ligand along with that of Dst is also shown for comparison in Figure 1. It is apparent from the structures that both the ligands have the requisite electrostatic and H-bonding sites, like Dst, for potential noncovalent bonding with the bases of DNA. However, the mPD derivative (as also NSC 101327) would be expected to have a backbone curvature different from that of Dst, which might lead to different van der Waals and hydrogen-bonding interactions in comparison to Dst. Therefore, the mPD derivative might be a good model ligand to probe the role of backbone curvature of the ligand in the specificity of Dst–DNA interaction.

Materials and Methods

The mPD derivative was synthesized as the di-*p*-toluenesulfonate salt [by a procedure to be communicated separately (Rao and Sasisekharan)] and characterized by elemental analysis, mass spectroscopy, and IR and NMR spectroscopic methods. The HPLC analysis (data not shown) by means of a Lichrosorb RP-18 column using methanol as eluent showed that the final synthetic product was pure (side products less than 5%). So, no further purification of the product was attempted. Dst was a generous gift from F. Arcamone (Farmitalia Carlo Erba, Italy). The polynucleotides poly(dA-dT), poly(dG-dC), and poly(dG-^{5}MedC)[1] were from Pharmacia P-L Biochemicals. They were used without further purification. The calf thymus (CT) DNA was from Sigma Chemical Co. and was used after deproteination by phenol extraction and extensive dialysis against 20 mM NaCl solution, pH 7.1. All other reagents used were of analytical grade. Stock solution of mPD derivative was prepared in a methanol buffer mixture (30:70 v/v) because of its low solubility in water.

The concentrations of the ligands and DNAs are expressed in moles per liter. They were determined by using the following molar extinction coefficient (mM^{-1} cm^{-1}) values: ϵ_{260}[poly(dA-dT)] = 6.7, ϵ_{254}[poly(dG-dC)] = 8.4, ϵ_{260}[poly(dG-^{5}MedC)] = 6.9, ϵ_{260}(CT DNA) = 6.6 (Wells et al., 1970), ϵ_{260}[poly(A)·poly(U)] = 6.6, ϵ_{303}(Dst) = 33.0, and ϵ_{292}(mPD derivative) = 44.0. r', the input ratio of the concentrations of the ligand and nucleotide base pair, was used throughout. All experiments were carried out in 20 mM NaCl solution, pH 7.1, and at a room temperature of 20 °C. The absorption spectra were recorded with Shimadzu-160 and Hitachi-557 spectrophotometers. The circular dichroism (CD) spectra were recorded with a Jasco J-20C spectropolarimeter, and the data were processed by means of a DP500N data processor. The CD values were expressed as molar ellipticity, [Θ], as

$$[\Theta] = 100\Theta_{obsd}/lc \quad \text{deg cm}^2\ \text{dmol}^{-1}$$

where Θ_{obsd} is the observed ellipticity in degrees, l is the path length of the cell (in centimeters), 0.5 cm, and c is the concentration of the polynucleotide (or DNA) in nucleotide base phosphates. Each spectrum reported is an average of two runs. The fluorescence spectra were recorded in the ratio mode on a Hitachi 650-60 spectrofluorometer.

The apparent affinity constant (K_{app}) for mPD derivative–DNA interaction was evaluated from absorbance titration of the ligand (at 300 nm) by means of a Scatchard plot (Scatchard, 1949) of r/c_f against r according to the equation

$$r/c_f = K_0(n - r)$$

[1] Abbreviations: poly(dA-dT), double-stranded alternating copolymer poly(dA-dT)·poly(dA-dT); poly(dG-dC), double-stranded alternating copolymer poly(dG-dC)·poly(dG-dC); poly(dG-^{5}MedC), double-stranded alternating copolymer poly(dG-^{5}MedC)·poly(dG-^{5}MedC); poly($^2NH_2$-dA-dT), double-stranded alternating copolymer poly($^2NH_2$-dA-dT)·poly($^2NH_2$-dA-dT); poly(A)·poly(U), double-stranded homopolymer.

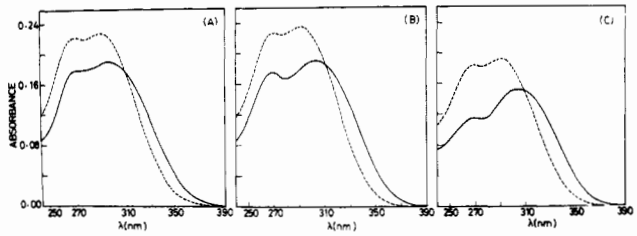

FIGURE 2: UV absorption spectrum of the mPD derivative alone (5.9 μM) (---) and in the presence of DNAs (118 μM) (—): (A) poly(dG-dC); (B) CT DNA; (C) poly(dA-dT). Note that in case of poly(dA-dT) the concentrations of the ligand and polymer are 5.6 and 112 μM, respectively.

where $r = c_b/c_p$ and c_b is the concentration of bound ligand, c_p is the input concentration of the DNA, c_f is the concentration of free ligand, K_0 is the intrinsic binding constant, and n is the binding stoichiometry.

K_{app} could be determined from known values of K_0 and n ($K_{app} = K_0 n$). K_{app} is the intercept of the straight line on the Y axis.

c_b was evaluated from the relation $c_b = \Delta A/\Delta\epsilon$, where ΔA denotes the decrease in absorbance (at 300 nm) of ligand due to the addition of DNA and $\Delta\epsilon = \epsilon_f - \epsilon_b$. ϵ_f is the extinction coefficient of the free ligand, and ϵ_b is the extinction coefficient of the bound ligand as measured from the absorbance of the ligand in the presence of a 50-fold excess of DNA.

Results and Discussion

Binding with DNA. The UV absorption spectrum of the compound is shown in Figure 2. The spectrum is characterized by the presence of peaks at 292 and 268 nm. It might be suggested that the long-wavelength peak arises from the extended conjugation involving the three benzene rings. This is supported by the earlier observation that the UV spectrum of another analogue of Dst, containing three benzene rings instead of pyrrole rings, also showed a peak around 292 nm (Dasgupta et al., 1986). The lower wavelength peak may be ascribed to the end pyridyl moieties (Silverstein et al., 1981).

The binding of the mPD derivative to polynucleotides poly(dA-dT) and poly(dG-dC) and calf thymus DNA is indicated from the change in its absorption spectrum in the presence of these polymers (Figure 2). A comparative study of the salient features of the spectra in the absence and presence of various DNAs suggests that, in general, a red shift of the long-wavelength peak ensues the polymer–ligand interaction. The extent of red shift follows the order poly(dA-dT) (14 nm) > CT DNA (11 nm) > poly(dG-dC) (7 nm). All spectra (in the presence of DNA) are characterized by crossover points at wavelengths that are different for the polynucleotides. Similar changes in the absorption spectrum of Dst in the presence of DNA were reported (Zimmer & Wahnert, 1986). The spectra of the synthetic analogues of Dst also exhibit similar kinds of changes in the presence of DNA (Dasgupta et al., 1986; Parrack et al., 1987). In analogy with the explanation offered earlier for the red shift of the peak of UV absorption spectrum of Dst (and the analogues) in the presence of DNA (Zimmer et al., 1971; Dasgupta et al., 1986, 1987), one might suggest that it occurs as a sequel to an enhanced degree (compared with the ligands alone) of conjugation of π electrons via the three benzene rings in the complex with DNA. It should, however, be noted that in contrast to Dst (Zimmer et al., 1971) or its synthetic analogues (Parrack et al., 1987) the magnitude of the changes in absorbance (at wavelength greater than 300 nm) of the mPD derivative upon binding with DNA is not significantly dependent on the base sequence (vide Figure 2). This is akin to what was reported for NSC 101327 (Luck et al., 1984). There is no significant shift of the peak at 268 nm in the spectrum of the mPD derivative upon its binding with DNA.

The formation of a complex between the mPD derivative and DNAs could be confirmed from the observation of an induced band (in 300–360-nm region) in the CD spectra of the ligand–DNA complexes such as shown in Figure 3. The ligand alone does not show any CD spectrum. Similar induced bands characterize the complex formation between Dst (or its synthetic analogues) and DNA (Zimmer, 1975; Dasgupta et al., 1986; Parrack et al., 1987). The representative CD spectra of the mixture of compound and DNAs [poly(dA-dT), CT DNA, and poly(dG-dC)] at two different ratios, $r' = 0.02$ and 0.1, are shown in parts A, B, and C of Figure 3, respectively.

The following features characterize the CD spectra of the complexes:

(i) There is an overlap of the band originating from induced asymmetry of the ligand and the band due to the polynucleotides and DNA.

(ii) The shapes are different for the induced bands in the cases of poly(dA-dT) and poly(dG-dC). For the poly(dA-dT)–mPD derivative complex, the broad envelope observed at $r' = 0.02$ appears as a distinct peak at 310 nm when $r' = 0.1$. In the mPD derivative–poly(dG-dC) complex, the flat

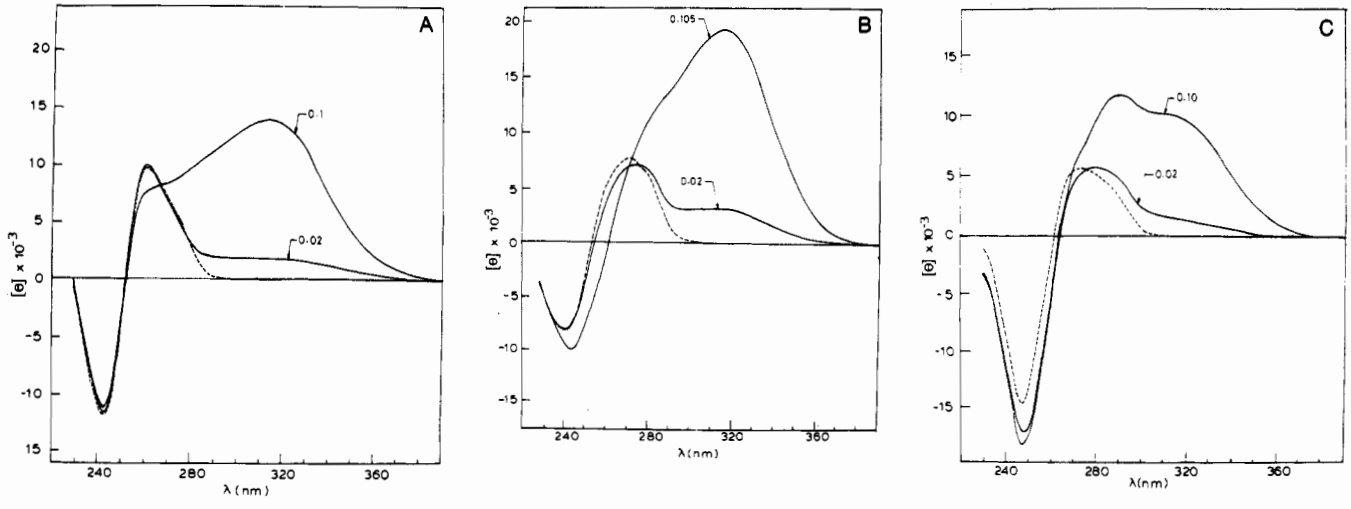

FIGURE 3: CD spectra of three DNAs (200 μM) in the absence (---) and presence (—) of mPD derivative at $r' = 0.02$ and 0.1: (A) poly(dA-dT); (B) CT DNA; (C) poly(dG-dC). The spectra corresponding to different input ratios are indicated by arrows, and the numbers beside the arrow state the ratio, r', corresponding to the spectrum.

Table I: Molar Ellipticity Values of Ligand–DNA Complexes[a]

complex	ionic strength (mM NaCl)	wavelength (nm)	molar ellipticity $[\Theta]^b$
Dst–poly(dA-dT)	20	318	36.0
Dst–poly(dA-dT)	200	318	35.5
Dst–poly(dG-dC)	20	318	5.0
Dst–poly(dG-dC)	200	318	0.75
mPD derivative–poly(dA-dT)	20	310	13.8
mPD derivative–poly(dA-dT)	200	310	13.0
mPD derivative–poly(dG-dC)	20	310	10.0
mPD derivative–poly(dG-dC)	200	310	8.8

[a] Measured at pH 7.1, 20 °C. The input ratio, r', of the concentrations of the ligand and DNA is 0.1. [b] Calculated as explained under Materials and Methods.

band in the 300–350-nm region at $r' = 0.02$ does not exhibit any definite peak at $r' = 0.1$. On the other hand, the CD spectrum of the complex with poly(dG-dC) (at $r' = 0.1$) is characterized by the presence of a peak at 285 nm.

(iii) The crossover point for the CD spectrum of the poly(dA-dT)–mPD derivative complex remains the same as observed in the polynucleotide alone, whereas a shift in the crossover point takes place in the case of the poly(dG-dC)–mPD derivative complex.

(iv) It is apparent from Figure 3B that the spectra of the complex with CT DNA (at $r' = 0.02$ and 0.1) contain the features of the spectra of the complexes of the ligand with poly(dA-dT) and poly(dG-dC). This probably indicates that the ligand binds to both A-T and G-C base pairs in the natural DNA.

(v) The overlap of the induced band and the positive band (at $r' = 0.1$) due to the polynucleotides makes it difficult to comment on the preservation of the conservative spectra of the polymers; however, it might be suggested that the interaction with the mPD derivative probably does not alter significantly the conservative CD spectra of the polymers.

(vi) The induced band (for $0 < r' \leq 0.3$) does not exhibit any significant change in its shape or intensity with the variation of the ionic strength of the medium from 20 to 200 mM NaCl. This behavior is similar to what has been reported for Dst–DNA complexes (Zimmer & Wahnert, 1986) and in contrast to the reversal of band observed in the case of NSC 101327 at an ionic strength of 0.1 M NaCl (for $r' \geq 0.2$) (Luck et al., 1984). Table I lists the values of the molar ellipticities (of the ligand–DNA complexes) at the peak wavelength of the induced band in the 300–350-nm region. For comparison, the values for the Dst–polynucleotide [poly(dA-dT) and poly(dG-dC)] complexes are also given. The ellipticity values are given at two extreme ionic strengths used in the experiment in order to demonstrate the influence of ionic strength, if any, upon them. It is apparent from the table that all the values with the lone exception of that for the Dst–poly(dG-dC) complex are relatively insensitive to the change in ionic strength. This trend is in accordance with the specific nature of the interactions between mPD derivative and polynucleotides. On the contrary, the band for the Dst–poly(dG-dC) complex at low ionic strength arises out of nonspecific association. Another comparative feature emerging from Table I is the higher strength of the band for the Dst–poly(dA-dT) complex with respect to that for the mPD derivative–poly(dA-dT) complex. This is probably a reflection of the inherent structural differences of the complex and the nature of the chromophoric groups in the ligands, Dst and mPD derivative.

Base Specificity of Binding. The base-sequence specificity of a ligand could be ascertained from the relative affinity of

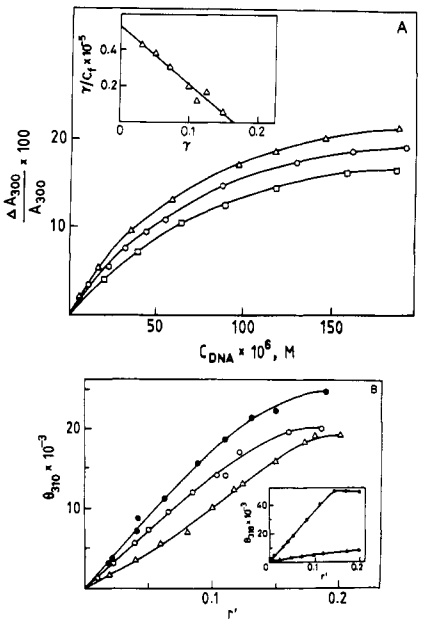

FIGURE 4: (A) Percent decrease in absorption at 300 nm for mPD derivative (6 μM) as a function of the input concentrations of different DNAs: poly(dA-dT) (○); CT DNA (△); poly(dG-dC) (□). Inset shows the representative Scatchard plot (r/c_f against r) for the evaluation of apparent binding constant for the interaction of mPD derivative and calf thymus DNA. (B) Variation of molar ellipticity (at 310 nm) ($[\Theta]_{310nm}$) of various DNAs as a function of r', the input ratio of the concentrations of mPD derivative and DNA (200 μM) poly(dA-dT) (○), poly(dG-dC) (△), and CT DNA (●); inset shows the variation of $[\Theta]_{318nm}$ of poly(dA-dT) (204 μM) and poly(dG-dC) (200 μM) as a function of r', the input ratio of the concentrations of the ligand, Dst, and polynucleotides poly(dA-dT) (○) and poly(pG-dC) (△).

Table II: Apparent Affinity Constants of mPD Derivative–DNA Complexes[a]

DNA	apparent affinity constant (K_{app})[b] (M^{-1})
poly(dA-dT)	4.8×10^4 (3.8×10^5)[c]
calf thymus DNA	5.6×10^4
poly(dG-dC)	4.1×10^4

[a] Measured at pH 7.1, 20 °C. [b] Calculated as explained under Materials and Methods. [c] Value in parentheses denotes K_{app} for the Dst–poly(dA-dT) interaction given for comparison (Dasgupta et al., 1987).

the ligand for DNAs of different base compositions. In the present case, the relative affinity of mPD derivative for DNAs of different base compositions was evaluated from the measurement of (i) changes in absorbance (at 300 nm) of the ligand as a function of the concentration of the added DNA and (ii) variation of the molar ellipticity (at 310 nm) of the induced band as a function of the input ratio r', for r' up to 0.2.

Figure 4A shows the percent change in absorbance of the mPD derivative as a function of the concentrations of different DNAs. For the sake of direct comparison of binding affinities, the concentration of mPD derivative has been kept constant in all cases. It is apparent from the curves that the concentrations of poly(dA-dT), calf thymus DNA, and poly(dG-dC) corresponding to half saturations are comparable. This indicates the comparable binding affinities of the ligand for poly(dA-dT), calf thymus DNA, and poly(dG-dC). However, the binding affinities were also calculated by means of Scatchard plots (Scatchard, 1949), the representative of which is shown (inset of Figure 4A) for calf thymus DNA. The affinity constants are summarized in Table II. The presence of a linear Scatchard plot in the case of calf thymus DNA consisting of both A-T and G-C base pairs further indicates

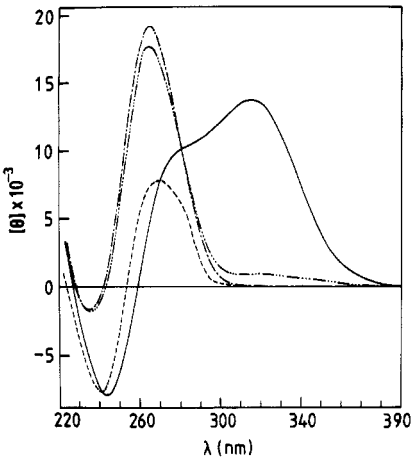

FIGURE 5: CD spectra of CT DNA (420 μM) in the absence and presence of mPD derivative (30 μM) in 20 mM NaCl solution, pH 7.1 under various conditions: CT DNA (--); CT DNA in the presence of mPD derivative (—); CT DNA in the presence of 75% v/v ethanol (---); CT DNA in the presence of 75% v/v ethanol and mPD derivative (-·--·-).

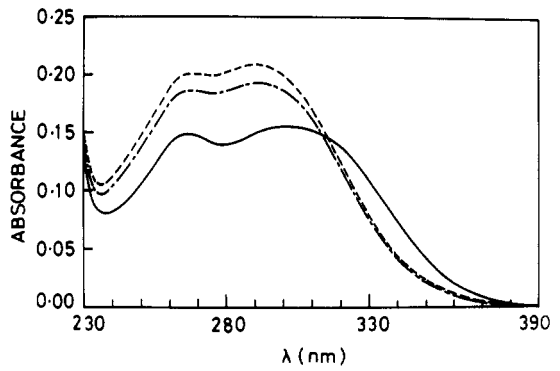

FIGURE 6: UV absorption spectra of mPD derivative alone (5.1 μM) (---) and in the presence of poly(dG-^{5}MedC) (31.4 μM) (—) and poly(dG-^{5}MedC) (31.1 μM) + $MgCl_2$ (4.8 mM) (---). Note the identical shape of the spectrum of mPD derivative in the absence of polynucleotide and in the presence of Mg^{2+} and polynucleotide. The little decrease in the absorbance of the mPD derivative in the presence of Mg^{2+} and poly(dG-^{5}MedC) can be accounted for by the dilution effect.

that the mPD derivative does not discriminate between the A-T and G-C base pairs in binding.

The relative affinity constants were also evaluated from the variation of molar ellipticity of the induced band under the condition when a fixed concentration of polynucleotide was titrated with varying amounts of the mPD derivative. Thus, the molar ellipticity at 310 nm is plotted as a function of the input ratio, r', for r' up to 0.2 (Figure 4B). The slopes of the curves associated with the binding of the ligand with poly(dA-dT) and poly(dG-dC) are not significantly different, thereby indicating that the mPD derivative probably does not exhibit any pronounced base selectivity in binding to poly(dA-dT) and poly(dG-dC). This is further apparent from the inset of Figure 4B, where a similar kind of plot of $[\Theta]_{318}$ against r' for Dst is shown for comparison; there is a marked difference in the slopes of the curves associated with Dst–poly(dA-dT) and Dst–poly(dG-dC) interactions. The slope of the binding curve associated with CT DNA–mPD derivative interaction further supports the conclusion that the mPD derivative does not exhibit any base selectivity. The slightly higher slope for the titration curves (both from UV absorbance and CD) in the case of calf thymus DNA could be ascribed to an enhanced affinity of mPD derivative for homopolymeric sequence such as poly(dA)·poly(dT).

The above experimental results definitely indicate that the mPD derivative does not exhibit any pronounced base selectivity in its association with DNA.

Dependence of Binding on the Nature of DNA Helix. The inability of the mPD derivative to bind to A-form DNA is suggested from the CD spectroscopic studies of its interaction with three different DNAs with the A-type structure.

(i) Figure 5 shows the absence of any significant induced band in the CD spectrum of calf thymus DNA when the latter is in A conformation under the influence of 75% v/v ethanol. For comparison, the strong induced band in the presence of B-form CT DNA is also shown.

(ii) No induced CD band could be observed when the CD spectrum of a mixture of mPD derivative and poly(A)·poly(U) (with A-form backbone structure) is recorded; neither could we observe any significant change in the absorption spectrum of the ligand upon the addition of poly(A)·poly(U) up to r' = 0.2 (figure not shown).

(iii) The binding to A-form DNA was also verified from the CD spectral analysis of the interactions of mPD derivative to poly($^2NH_2$dA-dT) under low-salt (20 mM NaCl) and high-salt (3 M NaCl) conditions. Concomitant with the B → A transition of the polynucleotide under high salt (3 M NaCl) (Borah et al., 1985), the induced CD band characterizing the complex formation under low-salt conditions disappears at a high salt concentration of 3 M NaCl (figure not shown). The resultant spectrum of the polymer is characteristic of inverted A-DNA form (Borah et al., 1985). This further suggests the absence of affinity for A-DNA type structure. This property is analogous to that of Dst and in contrast to that of NSC-101327.

The binding to Z-DNA was checked by two methods. As shown in Figure 6, the UV absorption spectrum of the mPD derivative undergoes changes in the presence of poly(dG-^{5}MedC) at low-salt condition (when the polynucleotide has B-DNA conformation). This change is similar to what has been observed for other B-DNAs like poly(dA-dT) or CT DNA, and it indicates binding of the ligand to the polynucleotide. Addition of exogeneous Mg^{2+} to this equilibrium mixture of mPD derivative and poly(dG-^{5}MedC) caused a reversal of the UV spectrum to that characteristic of the free ligand. This reversal of the spectrum of the mPD derivative indicates that the ligand does not bind to poly(dG-^{5}MedC) under the conditions favorable for its Z-DNA type conformation (Behe & Felsenfeld, 1981). The absence of the CD band in 300–350-nm region in the poly(dG-^{5}MedC)–mPD derivative complex under the condition when the polymer is in Z-form (in the presence of 25 mM $MgCl_2$) further supports its inability to bind to Z-form DNA (figure not shown). As a control experiment, an induced CD band in 300–350-nm region characterized the binding of mPD derivative to the B-form of poly(dG-^{5}MedC) in the absence of $MgCl_2$ (figure not shown). These experiments lend support to the conclusion that the mPD derivative does not recognize the Z form of the polynucleotide.

Binding to DNA via Minor Groove. The minor groove binding nature of the compound was indicated from the following two experiments. Dst, a well-established minor groove binding agent, was added to an equilibrium mixture of compound and poly(dA-dT). As evident from Figure 7A, progressive addition of Dst gives rise to the CD spectrum characteristic of the Dst–poly(dA-dT) complex, which is also shown for comparison in the figure. This suggests that Dst has progressively replaced the compound from its minor groove binding site. In a reverse experiment, the replacement of a well-known minor groove binding intercalating agent, ethidium

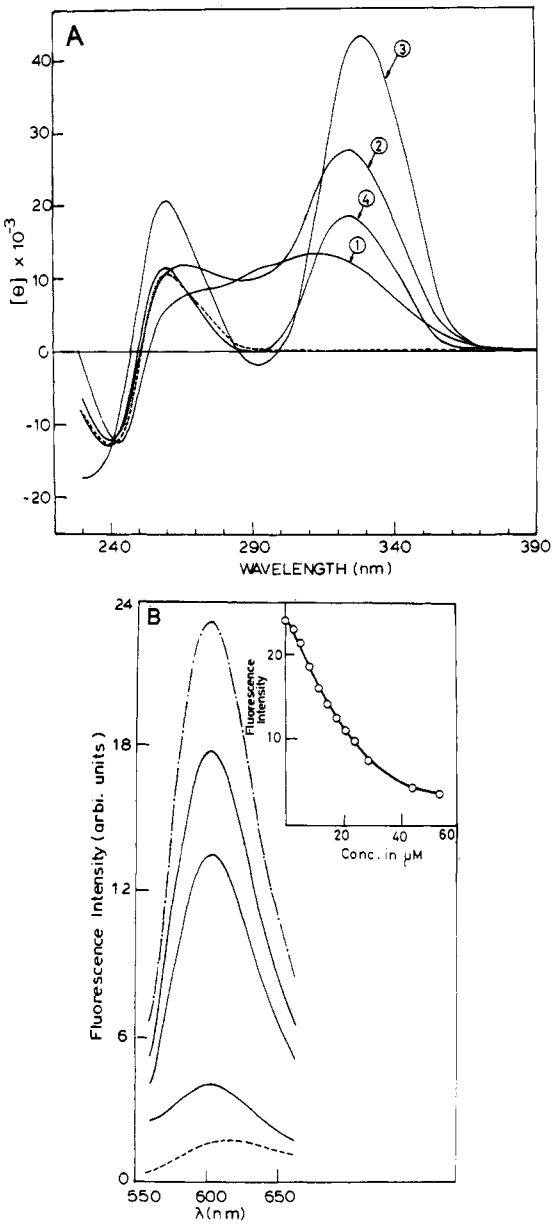

FIGURE 7: (A) Spectra of poly(dA-dT) (200 μM) alone (---), in the presence of mPD derivative (1) at $r' = 0.1$, and under the condition when distamycin was added at increasing concentrations of $r' = 0.05$ and 0.17 (2 and 3, respectively). For comparison the spectrum of poly(dA-dT) (203 μM) in the presence of distamycin alone at $r' = 0.065$ (4) is also shown. (B) Fluorescence emission spectra of ethidium bromide (6 μM) alone (---), in the presence of poly(dG-dC) (60 μM) (–·–), and upon addition of mPD derivative at different concentrations of 8.5, 14.8, and 44.3 μM (—). The spectra with decreasing intensity correspond to addition of increasing concentrations of mPD derivative. The inset shows the progressive decrease in the fluorescent emission intensity (at 600 nm) of the bound ethidium bromide as a function of the concentration of added mPD derivative. The excitation wavelength was fixed at 521 nm.

bromide, from its intercalation site in poly(dG-dC) is followed as a function of the added compound of mPD derivative (Baguley, 1982; Le Pecq & Paoletti, 1967). Figure 7B shows that there is a decrease in the fluorescence intensity indicative of the dissociation of ethidium bromide from poly(dG-dC) paralleling the addition of the mPD derivative to the equilibrium mixture of ethidium bromide and poly(dG-dC). Such replacement of ethidium bromide by the mPD derivative further supports its minor groove binding nature.

The physicochemical studies presented above lead to the following conclusion regarding the DNA-binding characteristics of the new compound. It binds via the minor groove to the B-form of DNA.

To summarize the above data, the comparative features of binding for the three ligands could be stated as follows: Dst, specific for A-T base pairs, only in B-helices (Zimmer & Wahnert, 1986); mPD derivative, nonspecific for base pairs but requires B-helices; and NSC 101327, nonspecific for base pairs and helix type (Luck et al., 1984).

Role of Curvature in the Ligand–DNA Interaction. It would be interesting to discuss the aforementioned comparative features of the binding of the three ligands, Dst, mPD derivative, and NSC 101327, in light of the backbone curvatures of the ligands. In order to emphasize the difference in backbone curvature, the torsion angles for the amide bonds are set to 0° or 180° (cis or trans) in all three cases (vide Figure 1). The X-ray analysis of the complex of netropsin with the B-DNA dodecamer of sequence (C-G-C-G-A-A-T-T-BrC-G-C-G) also suggests very minor deviation from planarity (Kopka et al., 1985).

It is apparent from Figure 1 that Dst has the maximum curvature among the three ligands. It might also be pointed out that the mPD derivative cannot be described by a single curvature with one radius; the H-bonding loci in this ligand are not spaced equidistantly.

In view of the above considerations about the structural features of the ligands, it might be commented that the backbone curvature probably plays a significant role in the observed differences in the specificities of their interactions with DNA. The backbone curvature would influence the van der Waals contact of the ligand with DNA and its amide orientation. However, the above differences in the specificity could also be due to the difference in π-system conjugations of the ligands.

The decrease in backbone curvature of the mPD derivative with respect to Dst has apparently led to the loss of A-T selectivity for a B-DNA-type conformation that characterizes the Dst–DNA interaction. Further decrease in backbone curvature from mPD derivative to NSC 101327 has resulted in loss of B-DNA backbone specificity as reflected in NSC 101327–DNA interaction (Luck et al., 1984). The recent theoretical analysis to understand the specificity of Dst– or Nt–DNA interaction also indicates the requirement for an appropriate curvature leading to steric fit of the ligand in the minor groove for favorable electrostatic and Lennard-Jones interaction energy. The formation of hydrogen bonds (between the potential sites of the ligand and bases of DNA) that also contributes to the energy of binding would be influenced by the backbone curvature of the ligand (Pullman, 1986; Zimmer & Wahnert, 1986). In light of these facts, the present investigation indicating the influence of curvature upon the DNA-binding specificity (of Dst- or Nt-type ligands) by means of an appropriate tailor-made ligand assumes further significance. Conformational analysis is under way in our laboratory to understand the role of curvature of these ligands upon their DNA-binding properties. However, any such analysis of the interaction with DNA to explain the salient features should consider the limitation of an isohelical analysis (Goodsell & Dickerson, 1986) of the interaction of this new ligand with DNA.

An important observation stemming from the present investigations is that the mPD derivative might be used as a probe for B-type structure in a DNA that contains sequence-dependent structural heterogeneity. The advantage of this ligand over the other presently available ligands is that it does not distinguish between A-T and G-C base pairs in a

B-DNA backbone. Currently, we are investigating the antibiotic properties of the new compound for its therapeutic potential.

ACKNOWLEDGMENTS

We thank Pradipkumar Parrack, Indira Chandrasekhar, and B. Gopalakrishnan for their help with the computer drawings of the backbone structures of the ligands, Dr. Probal Banerji for helping in synthesis, and Rajani Srinivasan and S. L. Nagaraj (Department of Biochemistry) for their technical assistance. We also thank the Department of Biochemistry for the use of CD spectropolarimeter and spectrofluorometer facilities. We gratefully acknowledge Prof. H. T. Miles, NIAAKD, Bethesda, MD, for the kind gift of poly($^2NH_2$-dA-dT) to Prof. V. Sasisekharan.

Registry No. Dst, 636-47-5; mPD, 113474-83-2; NSC 101327, 16758-33-1; poly(dG-^{5}MedC), 51853-63-5.

REFERENCES

Atwell, G. J., & Cain, B. F. (1968) *J. Med. Chem. 11*, 295-300.
Baguley, B. C. (1982) *Mol. Cell. Biochem. 43*, 167-181.
Behe, M., & Felsenfeld, G. (1981) *Proc. Natl. Acad Sci. U.S.A. 78*, 1619-1623.
Borah, B., Cohen, J. S., Howard, F. B., & Miles, H. T. (1985) *Biochemistry 24*, 7456-7462.
Dasgupta, D., Rajagopalan, M., & Sasisekharan, V. (1986) *Biochem. Biophys. Res. Commun. 140*, 626-631.
Dasgupta, D., Parrack, P., & Sasisekharan, V. (1987) *Biochemistry 26*, 6381-6387.
Goodsell, D., & Dickerson, R. E. (1986) *J. Med. Chem. 29*, 727-733.
Ivanov, V. I., Minchenkova, L. E., Minyat, E. E., Frank-Kamenetskii, M. D., & Schyolkina, A. K. (1974) *J. Mol. Biol. 87*, 817-833.
Kopka, M. L., Yoon, C., Goodsell, D., Pjura, P., & Dickerson, R. E. (1985) *Proc. Natl. Acad. Sci. U.S.A. 82*, 1372-1380.
Le Pecq, J. B., & Paoletti, C. (1967) *J. Mol. Biol. 27*, 87-106.
Lown, J. W., Krowicky, K., Bhat, U. G., Skorobogaty, A., Ward, B., & Dabrowiack, C. (1986) *Biochemistry 25*, 7408-7416.
Luck, G., Zimmer, Ch., & Baguley, B. C. (1984) *Biochim. Biophys. Acta 782*, 41-48.
Parrack, P., Dasgupta, D., Ayyer, J., & Sasisekharan, V. (1987) *FEBS Lett. 212*, 297-301.
Pullman, B. (1986) in *Molecular Mechanisms of Carginogenic and Antitumor Activity* (Pullman & Chagas, Eds.) Pontificiae Academiae Scientiarvm Documenta, Vatican Press.
Scatchard, G. (1949) *Ann. N.Y. Acad. Sci. 51*, 660-663.
Silverstein, R. M., Bassler, G. C., & Morrill, T. C. (1981) in *Spectrometric Identification of Organic Compounds*, p 329, Wiley, New York.
Wade, W. S., & Dervan, P. B. (1987) *J. Am. Chem. Soc. 109*, 1574-1575.
Wells, R. D., Larson, J. E., Grant, R. C., Shortle, B. E., & Cantor, C. R. (1970) *J. Mol. Biol. 54*, 465-497.
Zimmer, Ch. (1975) *Prog. Nucleic Acid Res. Mol. Biol. 15*, 285-318.
Zimmer, Ch., & Wahnert, U. (1986) *Prog. Biophys. Mol. Biol. 47*, 31-112.
Zimmer, Ch., Reinert, K. E., Luck, G., Wahnert, U., Lober, G., & Thrum, H. (1971) *J. Mol. Biol. 58*, 329-348.

Hairpin and Duplex Formation in DNA Fragments CCAATTTTGG, CCAATTTTTTGG, and CCATTTTTGG: A Proton NMR Study†

Pradip Pramanik, Neera Kanhouwa,‡ and Lou-sing Kan*
Division of Biophysics, SHPH, The Johns Hopkins University, 615 N. Wolfe Street, Baltimore, Maryland 21205
Received September 14, 1987; Revised Manuscript Received December 21, 1987

ABSTRACT: Three DNA fragments, CCAATTTTGG (**1**), CCAATTTTTTGG (**2**), and CCATTTTTGG (**3**), were studied by proton NMR spectroscopy in aqueous solution. All these oligodeoxyribonucleotides contain common sequences at the 5′ and 3′ ends (5′-CCA and TGG-3′). **2** as well as **3** forms only hairpin structures with four unpaired thymidylyl units, four and three base pair stems, respectively, in neutral solution under low and high NaCl concentrations. At high salt concentration the oligomer **1** forms a duplex structure with -TT- internal loop. On the other hand, the same oligomer forms a stable hairpin structure at low salt and low strand concentrations at pH 7. The hairpin structure of **1** has a stem containing only three base pairs (CCA·TGG) and a loop containing four nucleotides (-ATTT-) that includes a dissociated A·T base pair. The two secondary structures of **1** coexist in an aqueous solution containing 0.1 M NaCl, at pH 7. The equilibrium shifts to the hairpin side when the temperature is raised. The stabilities and base-stacking modes of all three oligonucleotides in two different structures are reported.

Hairpin loops in DNA, though rare, play an important role in gene control mechanisms (Muller & Fitch, 1982; Weaver & DePamphilis, 1984). Inverted repeat sequences in superhelical DNA extrude into cruciform structures (Sinden & Pettijohn, 1984; Frank-Kamenetskij & Vologodskij, 1984; Lilley, 1981; Sheflin & Kowalski, 1985) that appear to be involved in transcription and replication (Gierer, 1966). In hybridization experiments used in molecular cloning, short oligodeoxynucleotides are used. In the presence of appropriate complementary sequence and the low-concentration conditions used in hybridization experiments, hairpin loop formation may be important. A thorough knowledge of the conditions that favor loop formation is also expected to give a better under-

†This work was supported by NIH Grant GM 34252-08. Preliminary results of this work were presented at the Fifth Conversation in the Discipline of Biomolecular Stereodynamics, SUNY, Albany, NY, June 2-6, 1987.
‡Present address: Tufts University School of Medicine, Boston, MA.

0006-2960/88/0427-3024$01.50/0